Room-Temperature Rate Constant for the $HO_2 + HO_2$ Reaction at Low Pressures

Gerald A. Takacs[†] and Carleton J. Howard*[‡]

Aeronomy Laboratory, NOAA-R/E/AL2, Environmental Research Laboratories, Boulder, Colorado 80303
(Received: August 12, 1983)

The rate constant, k_1, for the self-reaction of HO_2, $HO_2 + HO_2 \rightarrow H_2O_2 + O_2$, was investigated in a discharge-flow system at room temperature and low pressures (1–7 torr) of He carrier gas by laser magnetic resonance detection of HO_2, OH, and NO_2. Three different chemical reactions, $F + H_2O_2$, $Cl + H_2O_2$, and $CH_2OH + O_2$, were used as sources of HO_2. Absolute concentrations of HO_2 were determined by converting HO_2 to OH and NO_2, by reaction with NO, and calibrating the system with known concentrations of OH or NO_2. The average values for k_1 in a phosphoric acid and halocarbon wax-coated flow tube were $(1.90 \pm \sigma = 0.05) \times 10^{-12}$ and $(1.54 \pm \sigma = 0.07) \times 10^{-12}$ cm^3 molecule^{-1} s^{-1}, respectively, at 295 ± 2 K, where the errors represent one standard deviation of the mean. These results indicate some effect from reactor surface coating. The recommended rate constant from this study is $k_1 = (1.5 \pm 0.3) \times 10^{-12}$ cm^3 molecule^{-1} s^{-1}, where the error is at the 95% confidence level and includes an estimate of systematic errors. This result combined with other recent studies indicates that the reaction has both pressure-independent and pressure-dependent mechanisms.

Introduction

The hydroperoxyl free radical, HO_2, is a vital chain carrier for chemical reactions that occur in atmospheric chemistry, combustion, and oxidation processes involving molecules that contain hydrogen.[1,2] HO_2 participates in all aspects of the mechanism of chain reactions: initiation via H abstraction by O_2; propagation by such reactions as $H + HO_2 \rightarrow 2OH$, $O + HO_2 \rightarrow OH + O_2$ and $OH + O_3 \rightarrow HO_2 + O_2$; and termination, for example, in $OH + HO_2 \rightarrow H_2O + O_2$ and

$$HO_2 + HO_2 \rightarrow H_2O_2 + O_2 \quad (1)$$

The kinetics of reaction 1, which is the sole known source of gaseous atmospheric H_2O_2, has been studied extensively at high pressures (~1 atm) and shows the interesting properties of a pressure dependence,[3,4] a negative temperature coefficient,[5–7] and a water-vapor dependence.[8,9] Most measurements at room temperature and 1-atm pressure find k_1, as defined by eq 2, in the range $(2.5–4.7) \times 10^{-12}$ cm^3 molecule^{-1} s^{-1}.[3–11]

$$-d[HO_2]/dt = 2k_1[HO_2]^2 \quad (2)$$

At low pressures (1–10 torr) there are fewer results and less agreement among investigators. In 1962 the first measurement of reaction 1 was given by Foner and Hudson[12] at 0.6 torr in a flow system with mass spectrometric detection of HO_2. Using sources and calibration procedures for HO_2 that were not well characterized, they reported an approximate value of $k_1 = 3 \times 10^{-12}$ cm^3 molecule^{-1} s^{-1}.

Thrush et al.[13] produced HO_2 by reactions 3 and 4 in a flow

$$F + H_2O_2 \rightarrow HF + HO_2 \quad (3)$$

$$k_3 = 8 \times 10^{-12} \text{ cm}^3 \text{ molecule}^{-1} \text{ s}^{-1}$$ [14]

$$Cl + H_2O_2 \rightarrow HCl + HO_2 \quad (4)$$

$$k_4 = 4.1 \times 10^{-13} \text{ cm}^3 \text{ molecule}^{-1} \text{ s}^{-1}$$ [2]

tube with several different wall surfaces including hydrofluoric acid cleaned Pyrex, Teflon, and a halocarbon wax. HO_2 decay was followed by laser magnetic resonance (LMR) detection, and a mean value of $k_1 = (7.5 \pm 5.0) \times 10^{-13}$ cm^3 molecule^{-1} s^{-1} was obtained with an argon carrier gas pressure between 1.9 and 2.9 torr. Thrush and Wilkinson[15] conducted similar experiments in a Teflon-coated flow tube and reported the following values for k_1 at various total pressures of helium carrier gas: $(2.9 \pm 1.2) \times 10^{-13}$ at 2 torr, $(4.3 \pm 1.8) \times 10^{-13}$ at 3 torr, and $(5.5 \pm 1.4) \times 10^{-13}$ cm^3 molecule^{-1} s^{-1} at 4 torr. These results extrapolate to $k_1 \simeq 0$ at $P = 0$ torr and imply purely termolecular behavior at low pressures. Assuming that their earlier results[13] for k_1 were proportional to the pressure of argon carrier, they corrected their mean value to $(7.4 \pm 3.3) \times 10^{-13}$ at 2.2 torr of argon.

Cox and Burrows[5] investigated reaction 1 in 3–760 torr of N_2 by a molecular modulation technique and found k_1 to be independent of pressure above 25 torr with a value of 2.5×10^{-12} cm^3 molecule^{-1} s^{-1}. These workers coated their reaction cell internally with a thin layer of PTFE Teflon to minimize heterogeneous removal of HO_2, which proved troublesome for their lower pressure experiments. Similarly, Lii et al.[11] using a pulse radiolysis method observed no pressure dependence over the range 400–1500 torr of H_2 and reported 3.1×10^{-2} cm^3 molecule^{-1} s^{-1} for k_1 at 298 K in their stainless-steel reaction cell.

The absorption spectrum of HO_2 was monitored following flash photolysis by Sander et al.[3] from 100–700 torr of He, Ar, N_2, O_2, and SF_6 and by Simonaitis and Heicklen[4] from 5 to 770 torr of N_2 and 50 to 500 torr of He. In contrast to the above investigations, both observed a pressure dependence for reaction 1. Their rate constants extrapolate to $k_1 \simeq 1.6 \times 10^{-12}$ cm^3 molecule^{-1} s^{-1} at $P = 0$ torr. These findings, as well as theoretical arguments,[16] suggest there is a pressure-dependent mechanism involving a weakly bonded H_2O_4 intermediate.

$$HO_2 + HO_2 \rightleftharpoons H_2O_4 \rightarrow H_2O_2 + O_2 \quad (5)$$

Thrush and Tyndall[17] formed HO_2 from reaction 6 by flash

$$CH_2OH + O_2 \rightarrow CH_2O + HO_2 \quad (6)$$

$$k_6 = 2 \times 10^{-12} \text{ cm}^3 \text{ molecule}^{-1} \text{ s}^{-1}$$ [18]

[†] NOAA-NRC Senior Research Associate, 1982–1983, on leave from Department of Chemistry, Rochester Institute of Technology, Rochester, New York.

[‡] Also affiliated with the Department of Chemistry, University of Colorado, Boulder, Colorado.

(1) C. J. Howard, "Proceedings of the NATO Advanced Study Institute on Atmospheric Ozone", Report No. FAA-EE 80-20, U.S. Department of Transportation, Washington, D.C., 1979.
(2) "Chemical Kinetics and Photochemical Data for Use in Stratospheric Modelling", Publication 82-57, National Aeronautics and Space Administration, Jet Propulsion Laboratory, Pasadena, CA, 1982.
(3) S. P. Sander, M. Peterson, R. T. Watson, and R. Patrick, *J. Phys. Chem.*, **86**, 1236 (1982).
(4) R. Simonaitis and J. Heicklen, *J. Phys. Chem.*, **86**, 3416 (1982).
(5) R. A. Cox and J. P. Burrows, *J. Phys. Chem.*, **83**, 2560 (1979).
(6) R.-R. Lii, R. A. Gorse, Jr., M. C. Sauer, Jr., and S. Gordon, *J. Phys. Chem.*, **83**, 1803 (1979).
(7) R. Patrick and M. J. Pilling, *Chem. Phys. Lett.*, **91**, 343 (1982).
(8) E. J. Hamilton, Jr., *J. Chem. Phys.*, **63**, 3682 (1975).
(9) E. J. Hamilton, Jr. and R.-R. Lii, *Int. J. Chem. Kinet.*, **9**, 875 (1977).
(10) T. T. Paukert and H. S. Johnston, *J. Chem. Phys.*, **56**, 2824 (1972).
(11) R.-R. Lii, R. A. Gorse, Jr., M. C. Sauer, Jr., and S. Gordon, *J. Phys. Chem.*, **84**, 813 (1980).
(12) S. N. Foner and R. L. Hudson, *Adv. Chem. Ser.*, **No. 36**, 34 (1962).
(13) J. P. Burrows, D. I. Cliff, G. W. Harris, B. A. Thrush, and J. P. T. Wilkinson, *Proc. R. Soc. London, Ser. A*, **368**, 463 (1979).
(14) D. J. Smith, D. W. Setser, K. C. Kim, and D. J. Bogan, *J. Phys. Chem.*, **81**, 898 (1977).
(15) B. A. Thrush and J. P. T. Wilkinson, *Chem. Phys. Lett.*, **66**, 441 (1979).
(16) R. Patrick, J. R. Barker, and D. M. Golden, *J. Phys. Chem.*, **88**, 128 (1984).

TABLE I: Injector Experimental Conditions[a]

source	$10^{-14}[X_2]$, cm^{-3}	$10^{-15}[H_2O_2]$, cm^{-3}	$10^{-14}[CH_3OH]$, cm^{-3}	$10^{-15}[O_2]$, cm^{-3}	$10^{-16}[He]$, cm^{-3}	$\bar{v}$, cm s^{-1}	$[X]/[X]_0$[b]	$[CH_2OH]/[CH_2OH]_0$[c]
$X + H_2O_2$ (X = F)	2.2–8.5	0.8–3.6			2.9–22.4	946–3419	$<6.1 \times 10^{-5}$	
$X + H_2O_2$ (X = Cl)	6.2–23.9	3.0–4.0			2.9–15.9	731–964	$<8.1 \times 10^{-4}$	
$X + CH_3OH + O_2$ (X = Cl)	0.5–9.3		2.8–25.2	2.6–11.5	1.9–12.8	486–3648	$<7 \times 10^{-12}$	$<3 \times 10^{-4}$

[a] Experimental conditions in the last 5 cm of the 7.0-mm-i.d. tube of the injector (Figure 1). [b] $[X]/[X]_0 = \exp\{-k_{X+Y}[Y]5/\bar{v}\}$ where X = Cl or F and Y = H_2O_2 or CH_3OH. [c] $[CH_2OH]/[CH_2OH]_0 = \exp\{-k_6[O_2]5/\bar{v}\}$.

TABLE II: Flow Tube Experimental Conditions

source	$10^{-14}[X_2]$, cm^{-3}	$10^{-15}[H_2O_2]$, cm^{-3}	$10^{-14}[CH_3OH]$, cm^{-3}	$10^{-15}[O_2]$, cm^{-3}	$10^{-16}[He]$, cm^{-3}	$\bar{v}$, cm s^{-1}	$10^{-12}[HO_2]$, cm^{-3}	$[HO_2]_i/[HO_2]_f$[a]
$X + H_2O_2$ (X = F)	0.7–2.7	0.4–1.2			3.1–22.9	302–367	0.9–14.5	1.7–6.7
$X + H_2O_2$ (X = Cl)	1.1–5.1	4.9–6.9			3.2–16.4	311–448	1.1–3.2	1.9–2.7
$X + CH_3OH + O_2$ (X = Cl)	0.4–0.9		1.5–7.8	1.1–2.7	3.0–12.9	329–397	1.0–11.8	2.1–4.6

[a] Ratio of initial to final HO_2 concentration that was observed over a 40-cm reaction distance.

photolysis of Cl_2–CH_3OH–O_2 mixtures and followed its decay with diode-laser spectroscopy in a quartz reactor. They found k_1 to be pressure independent from 7 to 20 torr of O_2 and in the range $(1.5–2.0) \times 10^{-12}$ cm^3 $molecule^{-1}$ s^{-1} at 308 K. Further measurements[19] yielded $k_1 = (1.6 \pm 0.1) \times 10^{-12}$ cm^3 $molecule^{-1}$ s^{-1} at 298 K.

In our investigation, a discharge-flow system was used to produce HO_2 by three different chemical sources: $F + H_2O_2$ (reaction 3), $Cl + H_2O_2$ (reaction 4), and $CH_2OH + O_2$ (reaction 6). LMR detection of HO_2, OH, and NO_2 permitted direct determination of k_1 at room temperature and low pressure (1–7 torr of He) in a flow tube with either phosphoric acid or halocarbon wax coatings.

Experimental Section

The flow tube reactor and the LMR technique for detecting HO_2, OH, and NO_2 with the 118.6-μm line of the water laser have been described in detail previously.[20,21]

The 2.54-cm i.d. Pyrex flow tube is double walled along the 60-cm reaction zone to provide temperature control by circulating either dibutyl phthalate (300–450 K) or ethanol (200–300 K) from a thermoregulated reservoir. The inside surface of the flow tube was coated with phosphoric acid or a halocarbon wax[22] (mp 405 K) and baked under vacuum at ~350 K to reduce the loss of radicals at the surface.

At the upstream end of the flow tube, a 1 m long, movable injector was placed inside of the flow tube and sealed to the flow tube with an O-ring as shown in Figure 1. The movable injector consisted of two coaxial Pyrex tubes; the inner tube was 4-mm i.d. while the outer was 7.0-mm i.d. The outer tube extended 5 cm beyond the end of the inner tube. An electrodeless microwave discharge cavity was attached to the top end of the movable inlet to generate the source atoms.

Fluorine atoms were made directly by discharging a He–F_2 mixture or indirectly by discharging a gas mixture containing a trace amount of H_2 in He to produce H atoms and adding a 10% F_2 in He mixture through the center inlet. Reactions 7 and 8 then

$$H + F_2 \rightarrow HF + F \quad (7)$$

$$k_7 = 1.6 \times 10^{-12} \text{ cm}^3 \text{ molecule}^{-1} \text{ s}^{-1}$$ [23]

$$F + H_2 \rightarrow HF + H \quad (8)$$

$$k_8 = 3.0 \times 10^{-11} \text{ cm}^3 \text{ molecule}^{-1} \text{ s}^{-1}$$ [24]

occur along the inner tube of the injector. Hydrogen peroxide

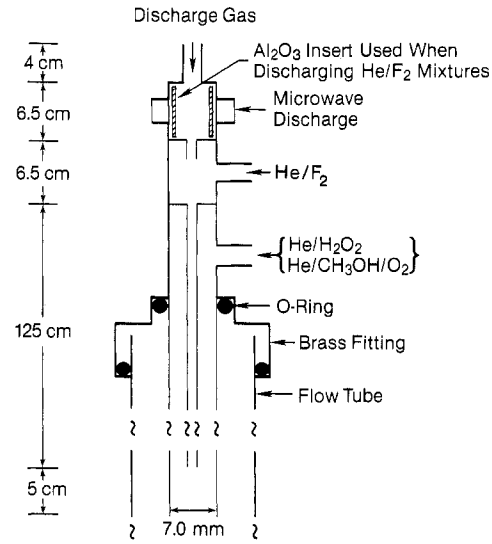

Figure 1. Triple-inlet movable injector.

was added through the third inlet of the injector, passed down the injector through the space between the inner and outer tubes, and reacted with F atoms via reaction 3 in the last 5 cm of the injector. Typical experimental conditions in the end of the injector are given in Table I. For these experimental conditions, pseudo-first-order loss of F atoms by reaction 3 (Table I) predicts that the fraction of F atoms exiting the injector was less than 6×10^{-5}.

When the $H + F_2$ reaction was used to produce F atoms, the subsequent rapid reaction of F with H_2, reaction 8, regenerates H. Therefore, small amounts of H are always present with this source. Low linear flow velocities and low H_2 concentrations were used in the experiments when F atoms were produced by $H + F_2$ in order to keep the concentration of H at a low level in the flow tube. Hydroxyl radicals were formed by $H + HO_2 \rightarrow 2OH$ and were removed by reactions 9 and 10 in the injector. These complications limited the usefulness of the $H + F_2$ source.

$$OH + HO_2 \rightarrow H_2O + O_2 \quad (9)$$

$$k_9 = 7 \times 10^{-11} \text{ cm}^3 \text{ molecule}^{-1} \text{ s}^{-1}$$ [2]

$$OH + H_2O_2 \rightarrow H_2O + HO_2 \quad (10)$$

$$k_{10} = 1.7 \times 10^{-12} \text{ cm}^3 \text{ molecule}^{-1} \text{ s}^{-1}$$ [2]

When F atoms were made by discharging He–F_2 mixtures, the concentration ratio of OH to HO_2 that was measured in the flow tube ranged from 6.2×10^{-6} to 1.6×10^{-4} and typically was $\sim 5 \times 10^{-5}$. At these OH concentration levels, reactions 9 and 10 have

(17) B. A. Thrush and G. S. Tyndall, *J. Chem. Soc., Faraday Trans. 2*, **78**, 1469 (1982).
(18) H. E. Radford, *Chem. Phys. Lett.*, **71**, 195 (1980).
(19) B. A. Thrush and G. S. Tyndall, *Chem. Phys. Lett.*, **92**, 232 (1982).
(20) (a) C. J. Howard and K. M. Evenson, *Geophys. Res. Lett.*, **4**, 437 (1977); (b) *J. Chem. Phys.*, **61**, 1943 (1974).
(21) M. S. Zahniser and C. J. Howard, *J. Chem. Phys.*, **73**, 1620 (1980).
(22) (a) G. A. Takacs and G. P. Glass, *J. Phys. Chem.*, **77**, 1060, 1182, 1948 (1973); (b) R. B. Badachhape, P. Kamarchik, A. P. Conroy, G. P. Glass, and J. L. Margrave, *Int. J. Chem. Kinet.*, **8**, 23 (1976).
(23) K. H. Homann, H. Schweinfurth, and J. Warnatz, *Ber. Bunsenges. Phys. Chem.*, **81**, 724 (1977).
(24) R. F. Heidner, J. F. Bott, C. E. Gardner, and J. E. Melzer, *J. Chem. Phys.*, **72**, 4815 (1980).

a negligible effect on the measurement of the rate of reaction 1.

The flow tube conditions (Table II) were such that the $[HO_2]$ changed by up to a factor of 6.7 over a 40-cm reaction distance. The possibility that part of the HO_2 decay may be due to a reaction between HO_2 and F_2 was investigated by producing small amounts of HO_2 on a side arm of the flow tube from the reaction $H + O_2 + M \rightarrow HO_2 + M$ (see Appendix for details) and adding excess F_2 through the injector. An upper limit of 2×10^{-16} cm^3 molecule^{-1} s^{-1} was found for the rate constant for the reaction between HO_2 and F_2, which contributed a negligible loss of HO_2 compared to that of reaction 1. Reaction between F_2 and H_2O_2 produced trace amounts of HO_2 with a rate constant $\leq 2 \times 10^{-16}$ cm^3 molecule^{-1} s^{-1}. The rate of production of HO_2 from $F_2 + H_2O_2$ is very slow compared to that from $F + H_2O_2$ under our experimental conditions and would produce a minor perturbation on the measured rate constant, k_1. With the above experimental parameters, a maximum production rate for HO_2 in the inlet tube of $\simeq 5 \times 10^{16}$ molecule s^{-1} was achieved with the $F + H_2O_2$ source.

The $Cl + H_2O_2$ experiments were similar to the $F + H_2O_2$ studies. A 4.8% Cl_2 in He mixture was passed through the discharge, and the resulting chlorine atoms were reacted with H_2O_2 in the end of the injector (Figure 1). For these experiments and the experiments involving $CH_2OH + O_2$, the injector surfaces exposed to Cl atoms below the discharge were coated with phosphoric acid to reduce the loss of chlorine atoms. The injector conditions (Table I) were such that the ratio $[Cl]/[Cl]_0$, as calculated solely on the pseudo-first-order loss of Cl by H_2O_2 (reaction 4), was in the range $(0.5–8.1) \times 10^{-4}$. Because of the complex chemistry of this system, a computer simulation of its kinetics was carried out for both the injector and the flow tube.

Reactions 11 and 12 were found to occur to a significant extent

$$Cl + HO_2 \rightarrow HCl + O_2 \quad (11)$$

$$k_{11} = 3.2 \times 10^{-11} \text{ cm}^3 \text{ molecule}^{-1} \text{ s}^{-1}$$ [25]

$$Cl + HO_2 \rightarrow ClO + OH \quad (12)$$

$$k_{12} = 9.1 \times 10^{-12} \text{ cm}^3 \text{ molecule}^{-1} \text{ s}^{-1}$$ [25]

in the injector (details are given in the Results section). Hydroxyl radicals, formed in reaction 12, are primarily removed by reaction with H_2O_2 (reaction 10) in the injector. The concentration ratio $[OH]/[HO_2]$ was measured to be in the range $(0.2–1.8) \times 10^{-4}$ in the flow tube. This confirmed the model predictions of negligible effects by OH on $[HO_2]$ along the length of the flow tube due to reactions 9 and 10. However, the ClO produced in reaction 12 contributed to HO_2 loss during the kinetic investigation via reaction 13 and affected the calibration procedure due to the

$$ClO + HO_2 \rightarrow HOCl + O_2 \quad (13)$$

$$k_{13} = 5.0 \times 10^{-12} \text{ cm}^3 \text{ molecule}^{-1} \text{ s}^{-1}$$ [2]

formation of Cl and NO_2 in reaction 14. The overall effects of

$$ClO + NO \rightarrow Cl + NO_2 \quad (14)$$

$$k_{14} = 1.7 \times 10^{-11} \text{ cm}^3 \text{ molecule}^{-1} \text{ s}^{-1}$$ [2]

reactions 13 and 14 on kinetic measurements of (1) were found to nearly compensate one another by computer modeling the chemistry and are described in the Results section. The maximum production rate of HO_2 that was obtained in the inlet tube from the $Cl + H_2O_2$ source was $\simeq 1 \times 10^{16}$ molecule s^{-1}. This production rate allowed the $[HO_2]$ to change by a factor of up to 2.7 during the kinetic study with flow tube conditions listed in Table II. No analogous problems occur with the $F + H_2O_2$ source because the fluorine reaction corresponding to (12) is endothermic.

Varying the $[Cl_2]$ by a factor of 4.6 had no measurable effect on the rate constant k_1, and therefore any loss of HO_2 by a reaction between HO_2 and Cl_2 was very small. An attempt at measuring the rate constant for $HO_2 + Cl_2$ placed the rate constant at $\leq 3 \times 10^{-15}$ cm^3 molecule^{-1} s^{-1}. Production of HO_2 by a reaction between Cl_2 and H_2O_2 was shown to occur with a rate constant $\leq 1 \times 10^{-17}$ cm^3 molecule^{-1} s^{-1}, and this reaction would have a minor effect on the measured value of k_1.

The hydrogen peroxide solution was prepared by evaporation under vacuum about 50% of an aqueous solution of 90 wt % H_2O_2 at room temperature. This increased the mole fraction of H_2O_2 in the residual solution to 92 ± 1% as determined from both measurements of the total vapor pressure and the partial pressure of H_2O_2, $P_{H_2O_2}$, above the solution.[26] $P_{H_2O_2}$ was measured by passing vapor from the solution through a 50-cm path absorption cell. The H_2O_2 cross section was taken as 3.2×10^{-19} cm^2 at the 213.9-nm Zn line.[27] A 25-nm (fwhm) interference filter was used in front of the Zn lamp to select the 213-nm radiation. The hydrogen peroxide flow rate, $F_{H_2O_2}$, was calculated from a measured flow of He through the absorption cell, F_{He}, the total pressure in the cell, P_A, the hydrogen peroxide partial pressure, and the mole fraction of H_2O_2 in the gas phase above the H_2O_2 solution, χ; $F_{H_2O_2} = F_{He}P_{H_2O_2}/(P_A - P_{H_2O_2}/\chi)$. For our purified H_2O_2 solution, χ equals 0.69 at 298 K,[26] the temperature at which H_2O_2 was used in our study. When not being used, the H_2O_2 solution was stored at ≤ 273 K. The $F_{H_2O_2}$ was not critical to the measurement of k_1, except for some modeling of the experiments. We estimate that $F_{H_2O_2}$ measurements were made with an accuracy of about ±20%.

The presence of H_2O in the H_2O_2 causes some complication because its reaction with fluorine atoms is fairly fast

$$F + H_2O \rightarrow HF + OH \quad (15)$$

$$k_{15} = 1.1 \times 10^{-11} \text{ cm}^3 \text{ molecule}^{-1} \text{ s}^{-1}$$ [2,28]

and produces OH which can further react with HO_2 (reaction 9) and H_2O_2 (reaction 10). However, as noted above, under the injector conditions used little OH entered the flow tube and reactions 9, 10, and 15 were limited to the volume within the injector. The analogous Cl reaction between Cl atoms and H_2O is endothermic and is too slow to be significant.

The third method for preparing HO_2 involved reacting chlorine atoms with a gaseous methanol–oxygen mixture (reaction 16

$$Cl + CH_3OH \rightarrow HCl + CH_2OH \quad (16)$$

$$k_{16} = 6.3 \times 10^{-11} \text{ cm}^3 \text{ molecule}^{-1} \text{ s}^{-1}$$ [29]

followed by 6 at the end of the inner tube of the injector (Figure 1). The experimental conditions in the injector were established so that reactions 16 and 6 were essentially complete within the injector tube (Table I). The Cl atoms were carried down the center tube of the injector by a stream of He while CH_3OH and O_2 passed through the space between the two tubes. The flow conditions (Table II) permitted measurements of HO_2 decays up to a factor of 4.6. Measurements of the concentration ratio of OH to HO_2 during the kinetic experiments ranged from 3.6×10^{-5} to 1.2×10^{-3}, indicating that little secondary chemistry such as the reaction of OH with CH_3OH

$$OH + CH_3OH \rightarrow H_2O + CH_2OH \text{ (or } CH_3O) \quad (17)$$

$$k_{17} = 1.0 \times 10^{-12} \text{ cm}^3 \text{ molecule}^{-1} \text{ s}^{-1}$$ [30]

followed by reaction 6 or the reaction of OH with HO_2 was occurring. The maximum production rate of HO_2 from the $Cl + CH_3OH + O_2$ source that was obtained, by using the above experimental conditions, was $\simeq 4 \times 10^{16}$ molecule s^{-1}.

To obtain the rate constant for reaction 1, absolute calibrations of the HO_2 LMR signal were required. Absolute concentrations were obtained by converting HO_2 to NO_2 and OH, by reaction

(25) Y.-P. Lee and C. J. Howard, *J. Chem. Phys.*, **77**, 756 (1982).

(26) "Hydrogen Peroxide Physical Properties Data Book", 3rd ed., FMC Corp., New York, 1969.

(27) Average of interpolated cross sections obtained from: (a) C. L. Lin, N. K. Rohotgi, and W. B. DeMore, *Geophys. Res. Lett.*, **5**, 113 (1978); (b) L. T. Molina, S. D. Schnike, and M. J. Molina, *ibid.*, **4**, 580 (1977); (c) L. T. Molina and M. J. Molina, *J. Photochem.*, **15**, 97 (1981).

(28) C. Zetzsch, Ph.D. Dissertation, Georg-August University, Gottingen, West Germany, 1971; reported in W. E. Jones and E. G. Skolnik, *Chem. Rev.*, **76**, 563 (1976).

(29) J. V. Michael, D. F. Nava, W. A. Payne, and L. F. Stief, *J. Chem. Phys.*, **70**, 3652 (1979).

(30) A. R. Ravishankara and D. D. Davis, *J. Phys. Chem.*, **82**, 2852 (1978).

with NO (reaction 18), and calibrating the system with known

$$HO_2 + NO \rightarrow OH + NO_2 \quad (18)$$

$$k_{18} = 8.3 \times 10^{-12}\ cm^3\ molecule^{-1}\ s^{-1}\ ^{2}$$

amounts of NO_2 or OH. Known amounts of OH were made from the reaction of excess H atoms with measured NO_2 concentrations via reaction 19. Details of the calibration procedures are given in the Appendix.

$$H + NO_2 \rightarrow OH + NO \quad (19)$$

$$k_{19} = 1.3 \times 10^{-10}\ cm^3\ molecule^{-1}\ s^{-1}\ ^{31}$$

Linear flow velocities of $\simeq 350$ cm s^{-1} (Table II) were used in the kinetic experiments to obtain maximum decays in $[HO_2]$. Since the calibrations were usually made at higher linear flow velocities, corrections were made for the change in the detection conditions. The corrections were determined by comparing the sensitivity of the LMR to NO_2 at the two conditions. The corrections were largest at low pressures, about 12% at 1 torr and decreased to about 1% at 7 torr.

The first-order wall loss of HO_2

$$HO_2 + \text{wall} \xrightarrow{k_w} \text{products} \quad (20)$$

was measured periodically throughout the study at concentration levels for which reaction 1 would not contribute to HO_2 loss, and k_w was typically $\leq 0.4\ s^{-1}$. To test the effect of k_w on the kinetics of reaction 1, four experiments were carried out in a halocarbon wax coated flow tube at a total pressure of 1 torr on the same chemical system except that the initial $[HO_2]$, $[HO_2]_0$, was varied. The $[HO_2]$ in these experiments changed by factors of 2.3, 3.0, 3.6, and 4.0 which corresponded to changes in $2k_1[HO_2]$ between 4 and 22 s^{-1}. The measured rate constants were within 1% of each other, indicating a negligible first-order wall effect on the kinetics. Some computer simulation calculations were performed using the GEAR program, which is a package of subroutines for the numerical solution of systems of ordinary differential equations.[32] A computer simulation of the system ($k_1 = 1.65 \times 10^{-12}$ cm^3 $molecule^{-1}$ s^{-1}, $k_w = 0.4\ s^{-1}$, $[HO_2]_0 = 5.1 \times 10^{12}\ cm^{-3}$, $\bar{v} = 347$ cm s^{-1}, $\Delta z = 40$ cm, and with integration step sizes $\leq 6 \times 10^{-5}$ s) showed the $[HO_2]$ would decay by a factor 3.0, corresponding to a change in $2k_1[HO_2]$ from 16.8 to 5.6 s^{-1}. A second-order plot of $1/[HO_2]$ against reaction distance gave $k_1 = 1.72 \times 10^{-12}$ cm^3 $molecule^{-1}$ s^{-1}, which is equivalent to a maximum wall effect of 5% on the measured rate constant. Since k_w was usually immeasurably small, no correction was made for first-order wall loss of HO_2.

The NO reactant was purified by passing it through a silica gel trap cooled with a dry ice–ethanol bath. NO_2 was prepared from the reaction of NO with excess O_2 at a pressure of about 900 torr. The NO_2 was kept at 0 °C when in use and stored at dry ice–ethanol temperature where it was a white solid. A small flow of He ($\sim$0.5 STP cm^3 s^{-1}) was added to the NO and NO_2 reactant flows to flush them through the inlet lines. Helium (analyzed >99.999%) was passed through molecular sieves at 77 K. CH_3OH (>99.5%), 4.8% Cl_2 in He, 10% F_2 in He, C_2F_3Cl, O_2 (>99.95%), and H_2 (>99.95%) were used without purification.

Results

Chemical Sources of HO_2. The principal limitation of the Cl + H_2O_2 source is that reaction 4, Cl + H_2O_2, which produces HO_2, is very slow compared to reactions 11 and 12, Cl + HO_2, which destroy HO_2. The linear flow velocities in the injector were kept low (731–964 cm s^{-1}), and the $[H_2O_2]$ maximized so that reaction 4 was complete (Table I) and the OH formed in reaction 12 was reacted. Reaction 12 also makes ClO, which as noted earlier, can interfere chemically in both the calibration procedure (reaction 14) and the kinetic measurement of HO_2 loss (reaction 13). The injector and flow tube chemistry were modeled to quantitatively examine these effects using a reaction scheme which included reactions 1, 4, 9–13, and 21–25. For the calibration experiments,

$$OH + HCl \rightarrow H_2O + Cl \quad (21)$$

$$k_{21} = 6.6 \times 10^{-13}\ cm^3\ molecule^{-1}\ s^{-1}\ ^{2}$$

$$ClO + OH \rightarrow Cl + HO_2 \quad (22)$$

$$k_{22} = 1.2 \times 10^{-11}\ cm^3\ molecule^{-1}\ s^{-1}\ ^{33}$$

$$ClO + ClO \rightarrow Cl + ClO_2 \quad (23)$$

$$k_{23} = 1.6 \times 10^{-14}\ cm^3\ molecule^{-1}\ s^{-1}\ ^{34}$$

$$ClO + ClO \rightarrow Cl_2 + O_2 \quad (24)$$

$$k_{24} = 7.8 \times 10^{-15}\ cm^3\ molecule^{-1}\ s^{-1}\ ^{34}$$

$$OH + HOCl \rightarrow H_2O + ClO \quad (25)$$

$$k_{25} = 1.8 \times 10^{-12}\ cm^3\ molecule^{-1}\ s^{-1}\ ^{2}$$

the additional reactions 14, 18, and 26 were added to the model

$$OH + C_2F_3Cl \rightarrow \text{products} \quad (26)$$

$$k_{26} = 6 \times 10^{-12}\ cm^3\ molecule^{-1}\ s^{-1}\ ^{35}$$

of the flow tube chemistry. The initial concentration of Cl atoms in the injector was not measured so it was estimated with the model by finding the amount that fitted the concentration of NO_2 in the computer simulation to that measured in the experiment. Under this condition the initial [Cl] corresponded to about 6% dissociation of the initial $[Cl_2]$, which agreed with other experiments where the Cl was detected. The model predicted that $\sim$75% of the measured NO_2 was made from HO_2. The remaining $\sim$25% of the NO_2 was made from ClO and NO by reaction 14 and from subsequent reactions involving the Cl atoms that are produced in reaction 14. Thus, the ClO had two effects which nearly cancel one another: (a) the ClO was converted to NO_2 and made the HO_2 concentration appear larger than it actually was during the calibration procedure, and (b) the ClO reacted rapidly with the HO_2, making the reaction rate too large. The net result was an error $\leq$–6% on the measured rate constant.

The Cl + CH_3OH + O_2 source was modeled by using reactions 6, 16, 17, 27–33, and all the chemistry used in modeling the Cl

$$Cl + CH_2O \rightarrow HCl + HCO \quad (27)$$

$$k_{27} = 7.3 \times 10^{-11}\ cm^3\ molecule^{-1}\ s^{-1}\ ^{2}$$

$$HCO + O_2 \rightarrow CO + HO_2 \quad (28)$$

$$k_{28} = 5.5 \times 10^{-12}\ cm^3\ molecule^{-1}\ s^{-1}\ ^{2}$$

$$Cl + HOCl \rightarrow Cl_2 + OH \quad (29)$$

$$k_{29} = 1.9 \times 10^{-12}\ cm^3\ molecule^{-1}\ s^{-1}\ ^{2}$$

$$Cl + O_2 + He \rightarrow ClOO + He \quad (30)$$

$$k_{30} = 1.0 \times 10^{-33}\ cm^6\ molecule^{-2}\ s^{-1}\ ^{2}$$

$$Cl + ClOO \rightarrow Cl_2 + O_2 \quad (31)$$

$$k_{31} = 1.4 \times 10^{-10}\ cm^3\ molecule^{-1}\ s^{-1}\ ^{2}$$

$$Cl + ClOO \rightarrow ClO + ClO \quad (32)$$

$$k_{32} = 8.0 \times 10^{-12}\ cm^3\ molecule^{-1}\ s^{-1}\ ^{2}$$

$$OH + CH_2O \rightarrow H_2O + HCO \quad (33)$$

$$k_{33} = 1.0 \times 10^{-11}\ cm^3\ molecule^{-1}\ s^{-1}\ ^{2}$$

(31) R. F. Hampson, "Chemical Kinetic and Photochemical Data Sheets for Atmospheric Reactions", Report No. FAA-EE-80-17, U.S. Department of Transportation, Federal Aviation Administration, Washington, D.C., 1980.

(32) A. C. Hindmarsh, "GEAR: Ordinary Differential Equation System Solver", Report No. UCID-30001, Revision 1, Lawrence Livermore Laboratory, University of California, Livermore, CA, Aug 20, 1972.

(33) A. R. Ravishankara, R. L. Eisele, and P. H. Wine, *J. Chem. Phys.*, **78**, 1140 (1983).

(34) R. D. Hudson, Ed., "Chlorofluoromethanes and the Stratosphere", NASA RP-1010, National Aeronautics and Space Administration, Washington, DC, Aug 1977.

(35) C. J. Howard, *J. Chem. Phys.*, **65**, 4771 (1976).

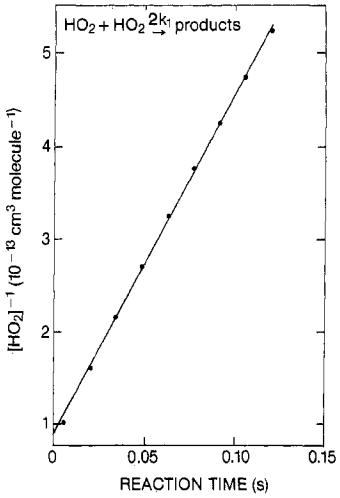

Figure 2. Plot of $1/[HO_2]$ against reaction time (source F + H_2O_2, phosphoric acid coated flow tube, $\bar{v}$ = 354 cm s^{-1}, P = 2.003 torr, and $k_1 = 1.87 \times 10^{-12}$ cm^3 $molecule^{-1}$ s^{-1}).

+ H_2O_2 source. With the experimental conditions listed in Table I, the [ClO] at the end of the injector was calculated to be $\leq 10^{-3}[HO_2]$, which in contrast to the Cl + H_2O_2 source, had a negligible effect on both the decay of HO_2 in the flow tube and on the production of NO_2 during the calibration. Similarly, the concentrations of other free radicals (e.g. Cl, OH, and HCO) were shown to be much lower in concentration than the [ClO] and they had an insignificant effect on $[HO_2]$ in the flow tube.

Making F atoms by reacting H atoms with F_2 (reaction 7) proved to be a less efficient method for production of HO_2 than by discharging F_2. The H atoms present in this system reacted rapidly with HO_2, $k = 7.4 \times 10^{-11}$ cm^3 $molecule^{-1}$ s^{-1},[36] producing OH and O which also react with HO_2. This secondary chemistry was confined to the injector tube by using low velocities in the injector which resulted in a lower HO_2 output with this source.

Rate Constant for HO_2 + HO_2. Rate constants for reaction 1 were obtained from the slopes of least-squares fits to plots of $1/[HO_2]$ against reaction time as illustrated in Figure 2. Several factors contributed to the scatter of the points in these decay plots. In some plots (such as Figure 2) there was a slight curvature caused by the failure of the movable inlet to stay perfectly aligned at the center of the flow tube as the inlet was moved. Also, the discharge source mounted on the upstream end of the movable inlet would have occasional fluctuations as the inlet was being moved. All of the plots were quite linear with the individual points falling well within a ±5% tolerance. All the values of k_1, from the various sources and calibration methods, are shown in Table III and plotted as a function of He carrier gas concentration in Figure 3.

The average values found for k_1, where the error limit is one standard deviation of the mean,[39] are $(1.90 \pm 0.05) \times 10^{-12}$ and $(1.54 \pm 0.07) \times 10^{-12}$ cm^3 $molecule^{-1}$ s^{-1}, respectively, for phosphoric acid and halocarbon wax coated flow tubes. There was no significant dependence of k_1 on He carrier gas pressure from 1 to 7 torr.

Discussion

The rate constant in a halocarbon wax coated flow tube, k_1 = 1.5×10^{-12} cm^3 $molecule^{-1}$ s^{-1}, was somewhat smaller than that obtained in a phosphoric acid coated flow tube, $k = 1.9 \times 10^{-12}$. Although some points from both sets of data overlap, we recom-

TABLE III: Measured Rate Constants for the HO_2 + HO_2 Reaction

source	calibration gas	$10^{-16}[M]$, cm^{-3}	$\bar{v}$, cm/s	$10^{12}k_1$, cm^3 $molecule^{-1}$ s^{-1}
Phosphoric Acid Coated Flow Tube				
Cl + CH_3OH + O_2	NO_2	6.50	397	2.10
	NO_2	9.75	353	1.81
	NO_2	3.26	385	2.26
	NO_2	3.28	336	1.60
Cl + H_2O_2	NO_2	3.32	414	1.73
	NO_2	6.53	448	1.94
	NO_2	9.75	372	2.01
	NO_2	13.3	311	2.14
	NO_2	16.3	369	1.93
	NO_2	16.5	330	1.87
F + H_2O_2	OH	6.52	360	1.87
	OH	13.1	338	1.95
	OH	3.24	306	1.76
	OH	9.80	302	1.57
	OH	16.4	348	1.82
	OH	23.0	348	2.07
				$1.90 \pm \sigma = 0.05$[a]
Halocarbon Wax Coated Flow Tube				
Cl + CH_3OH + O_2	NO_2	3.32	346	1.56
	NO_2	3.32	329	1.42
	NO_2	9.92	341	1.50
	NO_2	12.9	355	1.24
	NO_2	9.86	344	1.33
	OH	9.83	349	1.39
	OH	13.1	345	1.39
F + H_2O_2	OH	3.33	347	2.08
	OH	6.63	342	1.49
	OH	9.90	338	1.71
	OH	13.1	345	1.66
	OH	19.7	350	1.95
	OH	9.85	364	1.40
				$1.54 \pm \sigma = 0.07$[a]

[a] σ = standard deviation of the mean.

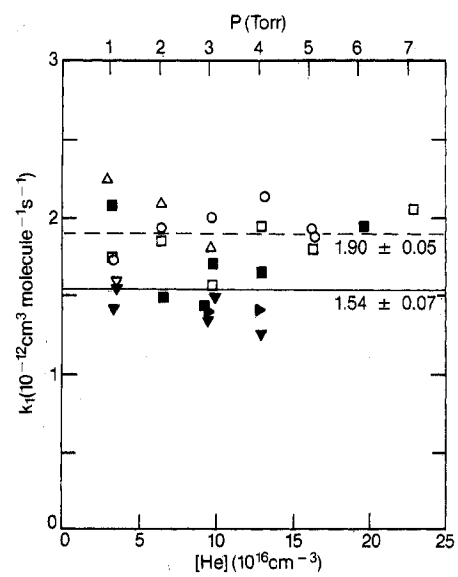

Figure 3. Rate constant for self-reaction of HO_2 as a function of He carrier gas concentration: △, Cl + CH_3OH + O_2, NO_2 calibration at kinetic conditions; ▽, Cl + CH_3OH + O_2, NO_2 calibration at high $\bar{v}$; ▷, Cl + CH_3OH + O_2, OH calibration; □, F + H_2O_2, OH calibration; ○, Cl + H_2O_2, NO_2 calibration at high $\bar{v}$. Open symbols represent the H_3PO_4 coated flow tube, and closed symbols represent the halocarbon wax coated flow tube.

(36) U. C. Sridharan, L. X. Qiu, and F. Kaufman, *J. Phys. Chem.*, **86**, 4569 (1982).

(37) The effect of the flow tube surface acting as a third body is observed at the [M] = 0 intercept in plots of the effective bimolecular rate constant vs. [M]. See for example: J. G. Anderson, J. J. Margitan, and F. Kaufman, *J. Chem. Phys.*, **60**, 3310 (1974); C. J. Howard, *J. Chem. Phys.*, **67**, 5258 (1977).

(38) Twenty-one measurements of k_1 in a wax-coated reactor at temperatures between 253 and 390 K fall on a line which gives $k_1 = 1.5 \times 10^{-12}$ cm^3 $molecule^{-1}$ s^{-1} at 295 K. Temperature dependence of the reaction HO_2 + HO_2 at low pressures: G. A. Takacs and C. J. Howard, in preparation.

(39) R. J. Cvetanovic, D. L. Singleton, and G. Paraskevopoulos, *J. Phys. Chem.*, **83**, 50 (1979).

mend that the lower rate constant be accepted as the preferred value. The 95% confidence limits on the mean rate constant for the two sets do not overlap so there is a statistically significant difference between the two data sets. It has been shown that HO_2 has a tendency to hydrogen bond strongly with H_2O and NH_3[2,8,9] and that the $HO_2 + HO_2$ reaction has a small termolecular component (this will be discussed more below). Flow tube studies of termolecular reactions often have a small second-order component which is due to a mechanism involving the wall as a third body.[37] We believe that the data taken with a phosphoric acid coating is more subject to an effect of this type than the data taken with the hydrophobic wax coating. Also, subsequent measurements directed toward determining the temperature coefficient of k_1 support the lower rate constant.[38]

The precision of our measurements was estimated by using the standard propagation of errors analysis given by Cvetanovic et al.[39] The errors associated with this estimate, which are all at the 95% confidence level, include the following: gas flow rates, ±3%; flow tube pressure, ±2%;, flow tube temperature, ±1%; flow tube radius, ±1%; decay plot slope, ±5%; and the HO_2 concentration calibration, ±15%. The resultant is ±17%. An additional factor, ±10%, for systematic errors raises the overall uncertainty to about ±20%. Although we know of no systematic errors, this factor is included to allow for the possibility of unknown reactions which might produce or destroy HO_2 and for possible errors in various calibrations. The standard deviation of the mean for the preferred halocarbon wax coating data set is about 5%, which gives a 95% confidence limit of about ±11%. We believe ±20% best represents a reasonable estimate of the accuracy of this measurement of k_1.

The observation of no significant pressure effect in this work confirms the recent data from Sander et al.[3] and Simonaitis and Heicklen.[4] These studies used flash-photolysis techniques to cover pressures from 100 to 700 torr and 5 to 770 torr, respectively, and a small termolecular component, $k_{N_2}^{III} \simeq 5 \times 10^{-32}$ cm^6 molecule^{-2} s^{-1}, was reported. If this is divided by two to allow for the lower M efficiency of He compared to that of N_2, we predict a change in k_1 of only about 5×10^{-15} cm^3 molecule^{-1} s^{-1} for the 6-torr pressure range of our measurements. This small increase in k_1 is far below the precision of our data. An effective low-pressure value of k_1 was given by extrapolation to $P = 0$ torr as $k_1^{II} = (1.6 \pm 0.2) \times 10^{-12}$ cm^3 molecule^{-1} s^{-1} by Sander et al.[3] and $(1.4 \pm 0.2) \times 10^{-12}$ by Simonaitis and Heicklen,[4] in excellent agreement with our result.

Thrush and Tyndall[17,19] have also published a low-pressure (7–20 torr) measurement, $k_1 = (1.6 \pm 0.1) \times 10^{-12}$ cm^3 molecule^{-1} s^{-1}, that agrees very well with ours. This result superceded the earlier data of Thrush and Wilkinson,[15] who reported a very large pressure effect at low pressure, but they gave no account for the origin of the discrepancy.

The major products of the self-reaction of HO_2 are $H_2O_2 + O_2$;[3,40] however, a recent study[41] gave evidence that H_2 is also produced:

$$HO_2 + HO_2 \rightarrow H_2 + 2O_2 \qquad (34)$$

These investigations are consistent with each other, if reaction 34 contributes ≤10% of the overall HO_2 loss. The formation of H_2 in reaction 34 has important consequences for the chemistry of the atmosphere. H_2 is a reservoir of hydrogen that has a much longer lifetime than H_2O_2 because it is less reactive with atmospheric radicals and it is not photolyzed. Therefore, H_2 can be transported to high altitudes where it is an important source of hydrogen radicals. The possible formation of H_2 requires further investigation.

Acknowledgment. This work was supported by the Chemical Manufacturers Association Technical Panel on Fluorocarbon Research and NOAA as part of the National Acid Precipitation Assessment Program. We thank A. J. Hills and J. R. McAfee for assistance with the GEAR computer program.

Appendix

HO_2 Calibration Procedures. The calibrations are made at concentrations which are about 5–20 times lower than those used in the kinetic measurements in order to eliminate complications from radical–radical reactions. Therefore, calibration procedures and the kinetic analysis assume that the HO_2 concentration is proportional to the LMR signal. The linearity of LMR detection of radicals was originally demonstrated for NO_2.[20b] Many tests have been made to show that the LMR detection method is linear for the stable paramagnetic gases NO and O_2, which can be added in accurately measured amounts. The linearity of OH and ClO detection have been demonstrated over a factor of 20–60 by rapid titration reactions, $H + NO_2$ and $Cl + O_3$, using measured amounts of NO_2 and O_3 in excess atoms. Also, the one to one conversion of HO_2 to OH has been established for a concentration range of about 100. In all cases no deviation from linearity was observed. The only exception to this rule is in some spectroscopic studies at very low pressures, <0.1 torr, saturation can occur. In the present studies the pressure was greater than 1 torr; therefore, we are confident that the assumption of linear detection is valid.

Calibration with OH. Low concentrations of HO_2 were produced by reaction 35 in a fixed side inlet located on the upstream

$$H + O_2 + He \rightarrow HO_2 + He \qquad (35)$$

end of the flow tube. The H atoms are reacted with O_2 in a high-pressure ($p \sim 20$ torr) cell,[21] and the high concentration of HO_2 in this cell effectively scavenges all the reactive impurities such as O, OH, and H so that only HO_2 (>99%) enters the flow tube from the source. Excess NO is then added through the injector when the injector is positioned just above the detection volume to stoichiometrically convert HO_2 to OH. In separate experiments the [OH] was calibrated by producing excess H atoms in a side inlet and adding known amounts of NO_2 through the injector under the same experimental conditions as the conversion of HO_2 to OH. Typically, the linear flow velocity used for this calibration was ≃1000 cm s^{-1}. Corrections for small differences in the calibration conditions and the kinetic experimental conditions were determined by measuring the LMR sensitivity to measured amounts of NO_2.

Calibration with NO_2. HO_2, produced from the $CH_2OH + O_2$ and $Cl + H_2O_2$ sources, was converted to NO_2 by reaction with excess NO. The OH product of reaction 18 was removed from the system because it destroyed HO_2 by reaction 9 or generated HO_2 from reactions 10 or 17 + 6. Therefore, as in previous studies from this laboratory,[20,21] C_2F_3Cl was added to the flow tube upstream of the injector outlet in order to scavenge OH by reaction 26. In the conversion experiments, the $[C_2F_3Cl]$ employed was such that the pseudo-first-order rate constant for reaction 26 was 24–290 times greater than those of the competing reactions $OH + H_2O_2$ or $OH + CH_3OH$.

In the study of the $F + H_2O_2$ source, significant amounts of HO_2 and OH were observed in undischarged mixtures of F_2–NO–H_2O_2 and F_2–C_2F_3Cl–H_2O_2 and therefore calibration could not be carried out accurately using NO_2.

The usual calibration procedure involved adding NO to convert HO_2 to NO_2 at low $[HO_2]$ and high linear flow velocities (~ 1600–1700 cm s^{-1}). Under these conditions, in the absence of NO, there was a very small change in the HO_2 signal due to reaction 1 along the 40-cm reaction distance. LMR measurements of HO_2 or NO_2 were then made at various reaction distances in the absence or presence of excess NO that was added directly into the detection volume. Some conversions were also done by adding the NO upstream of the injector outlet. The initial HO_2 signal that corresponded to the measured NO_2 signal was determined by extrapolation of the small HO_2 loss from the end of the injector to the detection volume. These corrections were typically in the range of 5–10%. With use of this latter procedure, the measured NO_2 signal was, within experimental error, constant over the

(40) F. Su, J. G. Calvert, C. R. Lindley, W. M. Uselman, and J. H. Shaw, *J. Phys. Chem.*, **83**, 912 (1979); H. Niki, P. D. Maker, C. M. Savage, and L. P. Breitenbach, *Chem. Phys. Lett.*, **73**, 43 (1980).

(41) K. A. Sahetchian, A. Hess, and R. Rigny, *Can. J. Chem.*, **60**, 2896 (1982).

40-cm reaction distance, indicating negligible loss of NO_2 along the flow tube.

A number of experimental tests, some of which are described here, were made to ensure that complications were not occurring in the above NO_2 calibration procedures. With the Cl + CH_3OH + O_2 source, in the absence of CH_3OH, significant amounts of NO_2 were produced from a mixture containing Cl, C_2F_3Cl, O_2, and NO. All four of these components were shown to be required in order to produce the NO_2 possibly by the following mechanism.

$$Cl + C_2F_3Cl \xrightarrow{M} C_2F_3Cl_2 \quad (36)$$

$$C_2F_3Cl_2 + O_2 \xrightarrow{M} C_2F_3Cl_2O_2 \quad (37)$$

$$C_2F_3Cl_2O_2 + NO \rightarrow C_2F_3Cl_2O + NO_2 \quad (38)$$

The possibility that a similar reaction sequence to (36)–(38) but involving OH instead of Cl atoms was shown not to occur to any measurable extent by reacting $[NO_2] \sim 2 \times 10^{13}$ cm^{-3} with H atoms in the last 5 cm of the injector and adding typical concentrations of C_2F_3Cl, CH_3OH, O_2, NO, and Cl_2 upstream of the injector outlet. The addition of these compounds produced no detectable NO_2. These experiments also ruled out the possibility that Cl atoms were being generated during the calibration procedure.

The reaction HO_2 + C_2F_3Cl was measured and found to be very slow by producing trace amounts of HO_2 by reaction 35 and adding C_2F_3Cl concentrations up to 6.8×10^{15} molecules cm^{-3} through the injector with a reaction time of 0.048 s. This sets an upper limit of $\leq 2 \times 10^{-16}$ cm^3 molecule^{-1} s^{-1} for HO_2 + C_2F_3Cl which is consistent with previous measurements.[20,21] A few kinetic experiments were also done with the Cl + CH_3OH + O_2 source when C_2F_3Cl was present to demonstrate that the OH + C_2F_3Cl adduct does not remove a significant amount of HO_2.

The possibility that some of the gases (CH_3OH, O_2, Cl_2, C_2F_3Cl, H_2O_2, and NO) may react with NO_2 was tested by adding these gases individually to a known concentration of NO_2. No evidence was observed for reaction of these gases with NO_2 under our experimental conditions. These findings are consistent with the reported rate constants for the reactions of NO_2 with CH_3OH ($k = 5.7 \times 10^{-37}$ cm^6 molecule^{-2} s^{-1})[42] and between NO_2 and H_2O_2 ($k \leq 1 \times 10^{-18}$ cm^3 molecule^{-1} s^{-1}).[43] Production of N_2O_3 from reaction of NO and NO_2 was also not expected because the equilibrium constant for $N_2O_3 \rightleftharpoons NO + NO_2$ is 1411 torr as calculated from thermochemical data.[44] Similarly, NO_2 dimerization in the flow tube is negligible for $[NO_2] \sim 1 \times 10^{13}$ molecules cm^{-3} at 298 K since $K_p = P_{NO_2}{}^2/P_{N_2O_4} = 106$ torr.[45]

After completion of the HO_2 to NO_2 conversion experiments, the microwave discharge that produced the Cl atoms was turned off. No NO_2 was produced by reactions between the gases, for the Cl + CH_3OH + O_2 and Cl + H_2O_2 sources, when the discharge was off. Known amounts of NO_2 were then added to calibrate for the response of the LMR to NO_2.

A few calibrations for HO_2 from the Cl + CH_3OH + O_2 source were performed at kinetic conditions. To account for the second-order loss of HO_2 between the end of the movable inlet and the detection volume, the effective reaction time was measured by using the slow reaction between HO_2 and NO_2.

$$HO_2 + NO_2 + He \rightarrow HO_2NO_2 + He \quad (39)$$

$$k_{39} = 1.0 \times 10^{-31} \text{ cm}^6 \text{ molecule}^{-2} \text{ s}^{-1}$$ [46]

All the calibration procedures described above gave good agreement. We estimate that the accuracy of our $[HO_2]$ measurements was about 15%.

Registry No. HO_2, 3170-83-0; F, 14762-94-8; Cl, 22537-15-1; CH_2OH, 2597-43-5; H_2O_2, 7722-84-1.

(42) H. Niki, P. D. Maker, C. M. Savage, and L. P. Breitenbach, *Int. J. Chem. Kinet.*, **14**, 1199 (1982).
(43) D. Gray, E. Lissi, and J. Heicklen, *J. Phys. Chem.*, **76**, 1919 (1972).
(44) D. R. Stull and H. Prophet, Eds., "JANAF Thermochemical Tables", National Bureau of Standards, Washington, D.C., 1971.
(45) R. J. Nordstrom and W. H. Chan, *J. Phys. Chem.*, **80**, 847 (1976).
(46) C. J. Howard, *J. Chem. Phys.*, **67**, 5258 (1977).

Fourier Transform Infrared Spectroscopic Study of the Kinetics for the HO Radical Reaction of $^{13}C^{16}O$ and $^{12}C^{18}O$

H. Niki,* P. D. Maker, C. M. Savage, and L. P. Breitenbach

Research Staff, Ford Motor Company, Dearborn, Michigan 48121 *(Received: August 29, 1983)*

The rate constants for the HO reaction of $^{13}C^{16}O$ and $^{12}C^{18}O$ were determined by the competitive kinetic method relative to that for the HO–C_2H_4 reaction, $k(HO+C_2H_4)$, in the presence of 700 torr of air at 299 ± 2 K. The HO radicals were generated in the photooxidation of RONO (R = CH_3 and C_2H_5). On the basis of FT IR spectroscopic measurements of the rates of C_2H_4 decay and formation of isotope-labeled CO_2 products, $k(HO+C_2H_4)/k(HO+{}^{13}C^{16}O)$ and $k(HO+C_2H_4)/k(HO+{}^{12}C^{18}O)$ were determined to be 35.95 ± 0.95(σ) and 36.30 ± 0.84, respectively. These values combined with $k(HO+C_2H_4) = (8.48 \pm 0.20(\sigma)) \times 10^{-12}$ cm^3 molecule^{-1} s^{-1} reported recently by Atkinson et al. give $k(HO+{}^{13}C^{16}O) = (2.36 \pm 0.12) \times 10^{-13}$ and $k(HO+{}^{12}C^{18}O) = (2.34 \pm 0.12) \times 10^{-13}$ cm^3 molecule^{-1} s^{-1}.

Introduction

Despite the well-recognized, critical role of the HO–CO reaction in atmospheric chemistry, there is still significant uncertainty concerning its rate constant, k(HO+CO), relevant at tropospheric conditions. Namely, several previous studies revealed dependence of k(HO+CO) on diluent pressure and on the presence of O_2.[1-7] Thus, the HO–CO reaction is presumably not a simple elementary reaction but may involve an addition complex which can yield HO_2 and CO_2 in the presence of O_2,[6,8] e.g.

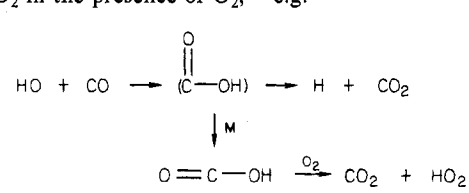

(1)

(1) Sie, B. K. T.; Simonaitis, R.; Heicklen, J. *Int. J. Chem. Kinet.* **1976**, *8*, 85.
(2) Cox, R. A.; Derwent, R. G.; Holt, P. W. *J. Chem. Soc., Faraday Trans. 1* **1976**, *72*, 2031.
(3) Overend, R.; Paraskevopoulos, G. *Chem. Phys. Lett.* **1977**, *49*, 109.
(4) Chan, W. H.; Uselman, W. M.; Calvert, J. G.; Shaw, J. H. *Chem. Phys. Lett.* **1977**, *45*, 240.
(5) Atkinson, R.; Perry, P. A.; Pitts, J. N., Jr. *J. Chem. Phys.* **1979**, *66*, 1197.
(6) Biermann, H. W.; Zetzsch, C.; Stuhl, F. *Ber. Bunsenges. Phys. Chem.* **1978**, *82*, 633.
(7) Butler, R.; Solomon, I. J.; Snelson, A. *Chem. Phys. Lett.* **1978**, *54*, 19.

0022-3654/84/2088-2116$01.50/0